AFRL-RX-WP-TP-2008-4308

APPLYING A PHYSICS-BASED DESCRIPTION OF FATIGUE VARIABILITY BEHAVIOR TO PROBABILISTIC LIFE PREDICTION (PREPRINT)

S.K. Jha, J.M. Larsen, and A.H. Rosenberger

Metals Branch
Metals, Ceramics, and NDE Division

JULY 2007

AIR FORCE RESEARCH LABORATORY
MATERIALS AND MANUFACTURING DIRECTORATE
WRIGHT-PATTERSON AIR FORCE BASE, OH 45433-7750
AIR FORCE MATERIEL COMMAND
UNITED STATES AIR FORCE

REPORT DOCUMENTATION PAGE

Form Approved
OMB No. 0704-0188

1. REPORT DATE *(DD-MM-YY)*	2. REPORT TYPE	3. DATES COVERED *(From - To)*
July 2007	Journal Article Preprint	

4. TITLE AND SUBTITLE
APPLYING A PHYSICS-BASED DESCRIPTION OF FATIGUE VARIABILITY BEHAVIOR TO PROBABILISTIC LIFE PREDICTION (PREPRINT)

5a. CONTRACT NUMBER
In-house

5b. GRANT NUMBER

5c. PROGRAM ELEMENT NUMBER
62102F

6. AUTHOR(S)
S.K. Jha (Universal Technology Corporation)
J.M. Larsen and A.H. Rosenberger (AFRL/RXLMN)

5d. PROJECT NUMBER
4347

5e. TASK NUMBER
RG

5f. WORK UNIT NUMBER
M02R3000

7. PERFORMING ORGANIZATION NAME(S) AND ADDRESS(ES)
Universal Technology Corporation
Metals Branch (AFRL/RXLMN)
Metals, Ceramics, and NDE Division
Materials and Manufacturing Directorate
Wright-Patterson Air Force Base, OH 45433-7750
Air Force Materiel Command, United States Air Force

8. PERFORMING ORGANIZATION REPORT NUMBER
AFRL-RX-WP-TP-2008-4308

9. SPONSORING/MONITORING AGENCY NAME(S) AND ADDRESS(ES)
Air Force Research Laboratory
Materials and Manufacturing Directorate
Wright-Patterson Air Force Base, OH 45433-7750
Air Force Materiel Command
United States Air Force

10. SPONSORING/MONITORING AGENCY ACRONYM(S)
AFRL/RXLMN

11. SPONSORING/MONITORING AGENCY REPORT NUMBER(S)
AFRL-RX-WP-TP-2008-4308

12. DISTRIBUTION/AVAILABILITY STATEMENT
Approved for public release; distribution unlimited.

13. SUPPLEMENTARY NOTES
Journal article submitted to *Engineering Fracture Mechanics*.

PAO Case Number: AFRL/WS 07-1597; Clearance Date: 09 Jul 2007. The U.S. Government is joint author of this work and has the right to use, modify, reproduce, release, perform, display, or disclose the work.

14. ABSTRACT
We describe fatigue lifetime variability as the separation/overlap of a crack-growth-controlled life-limiting mechanism and a mean-lifetime dominating behavior. We implement this description through a bimodal probability density representing the superposition of the crack growth and the mean-lifetime dominating densities. With the help of an a+b titanium alloy it is shown that the effect of microstructure, temperature, and loading variables on lifetime variability can be realized in terms of the degree of influence of these variables on the two densities affecting their separation and therefore, the total variability. We suggest that this behavior may be related to the development of a range of heterogeneity levels in a material at any given loading condition, which appears to present some probability of a predominately crack-growth controlled mechanism. A procedure, based on the new description of fatigue variability, for predicting the probability of failure from relatively small number of experiments is discussed.

15. SUBJECT TERMS
fatigue variability, life prediction, life-limiting mechanism, probability of failure, alpha + beta titanium, Ti-6Al-2Sn-4Zr-6Mo, crack initiation, crack growth

16. SECURITY CLASSIFICATION OF:			17. LIMITATION OF ABSTRACT:	18. NUMBER OF PAGES	19a. NAME OF RESPONSIBLE PERSON (Monitor)
a. REPORT	b. ABSTRACT	c. THIS PAGE			James M. Larsen
Unclassified	Unclassified	Unclassified	SAR	36	19b. TELEPHONE NUMBER *(Include Area Code)* N/A

Standard Form 298 (Rev. 8-98)
Prescribed by ANSI Std. Z39-18

Applying a "Physics-Based" Description of Fatigue Variability Behavior to Probabilistic Life Prediction

S. K. Jha*, J. M. Larsen, and A. H. Rosenberger

US Air Force Research Laboratory
AFRL/MLLMN
Wright-Patterson Air Force Base, OH – 45433

*Universal Technology Corporation
1270 N. Fairfield Road
Dayton, OH – 45432

ABSTRACT

We describe fatigue lifetime variability as the separation/overlap of a crack-growth-controlled life-limiting mechanism and a mean-lifetime dominating behavior. We implement this description through a bimodal probability density representing the superposition of the crack-growth and the mean-lifetime dominating densities. With the help of an α+β titanium alloy it is shown that the effect of microstructure, temperature, and loading variables on lifetime variability can be realized in terms of the degree of influence of these variables on the two densities affecting their separation and therefore, the total variability. We suggest that this behavior may be related to the development of a range of heterogeneity levels in a material at any given loading condition, which appears to present some probability of a predominantly crack-growth controlled mechanism. A procedure, based on the new description of fatigue variability, for predicting the probability of failure from relatively small number of experiments is discussed. This description appears to explain the fatigue variability trends with respect to operating variables reported in other studies and is shown to be especially relevant in decreasing the uncertainty in the useful-lifetime prediction.

Keywords: Fatigue variability, life prediction, life-limiting mechanism, probability of failure, α+β titanium, Ti-6Al-2Sn-4Zr-6Mo, crack initiation, crack growth

1. INTRODUCTION

The traditional description of fatigue variability behavior appears to be guided by the mean-lifetime response [1, 2]. This is schematically illustrated in Fig. 1. The lifetime probability-density is based on the deterministic understanding of the mean-fatigue relationship to operating variables and is commonly derived from probability distribution of variables in these relationships with respect their mean values [3, 4]. As illustrated in Fig. 1(a), an implicit assumption in this description is that the tails of the fatigue variability behavior result from random deviations from the overall mean behavior and have the same response to the operating variables as the mean. Sufficient number of experiments may not be always available, however, to verify this trend. Figure 1 also illustrates that the uncertainty in lifetime is often observed to increase with decreasing stress level, which is attributed to a greater contribution of the crack initiation regime in the total lifetime [5].

The current approach to life-management of fracture-critical components also seems to be driven by the above understanding of fatigue variability [1, 2]. As illustrated for a given loading in Fig. 1, the lower-tail and therefore the book-life is derived by extrapolation of variability with respect to the mean to an acceptable level of risk (typically taken as 1 in 1000 probability of development of a pre-defined level of damage) [6]. As such, this approach appears to present a significant uncertainty in life-prediction [6]. The underlying fatigue variability description in this approach may also produce physically counterintuitive predictions with respect to the operating variables. For example, due to increased uncertainty in lifetime with decreasing stress level, smaller useful-lifetimes may be predicted at lower stress levels as illustrated for the $\alpha+\beta$ titanium alloy, Ti-6Al-2Sn-4Zr-6Mo (Ti-6-2-4-6), in Fig. 2((a) and (b)) [7, 8]. The experimental points are plotted with respect to the lognormal cumulative distribution function (CDF) (shown by

broken lines) in Fig. 2(a). As the stress level was decreased the mean lifetime significantly increased (Fig. 2(a)) which is attributed to increased contribution from the crack initiation regime in α+β titanium alloys [9]. The increase in the mean corresponded to a shift in the upper-tail behavior to the right (Fig. 2(a)). On the other hand the life-limiting behavior or the lower-tail in Fig. 2(a) was very weakly affected by stress level. This produced an increased separation between the crack initiation-dominated mean-response, and the life-limiting behavior as illustrated by the bar graph in Fig. 2(b). Since the increased variability is attributed only to the deviation from the overall mean-response, the present understanding allows for arbitrarily increasing the scale of the lifetime-distribution function, therefore, resulting in a significantly lower design lifetime (the 1 in 1000, or the B0.1 lifetime shown in Fig. 2(b)) at lower stress levels.

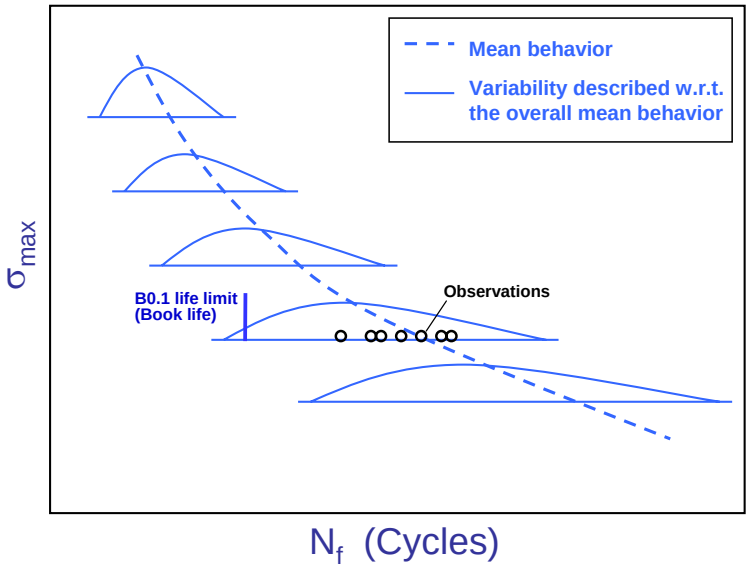

Fig. 1: Illustration of the traditional description fatigue variability behavior the corresponding life-prediction approach.

The same arguments as above can also be applied to the observed decrease in lifetime variability with an increase in the operating temperature [8] or by seeding a material with non-metallic particles which produces uniformly distributed crack initiation sites [10, 11]. In the

traditional description of fatigue variability, if the lifetime uncertainty in these cases is described only as deviations with respect to the mean behavior, it is possible to predict significantly lower B0.1 design lifetimes at the room temperature than at the elevated temperature. Similarly, a lower B0.1 limiting lifetime may be predicted in a relatively defect-free material when compared to increased defect content. These conclusions can be reasoned statistically, but from a physical standpoint one expects a greater risk of failure at elevated temperature and in the presence of defects.

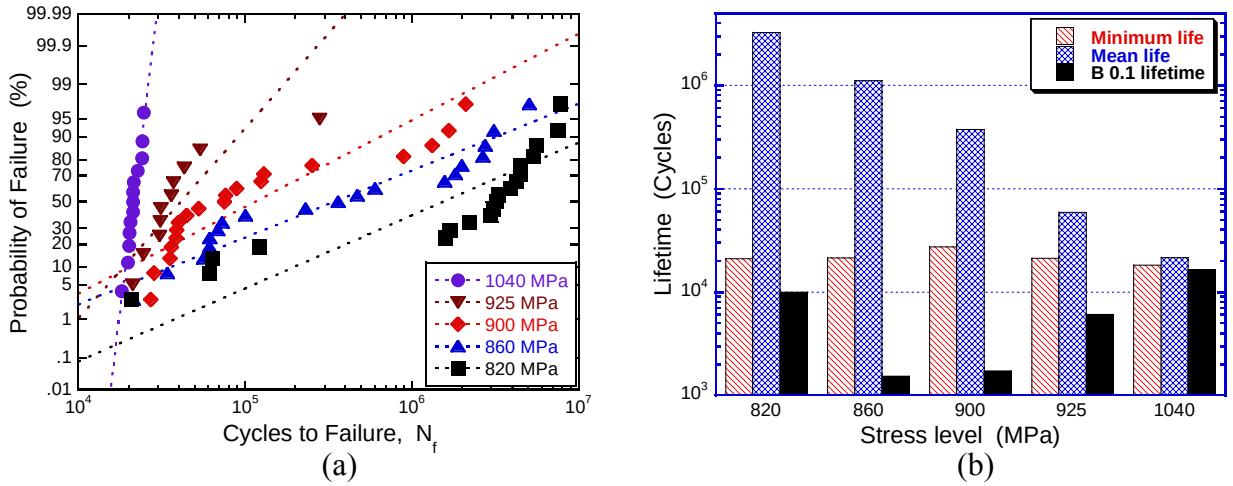

Fig. 2: Illustration of the separate response of tails and the mean of the fatigue variability behavior of Ti-6-2-4-6; (a) CDF vs. experiment and (b) Illustration of physically counterintuitive B0.1 lifetime w.r.t. stress level when based on the traditional description of fatigue variability.

The questions we seek to address in this paper are firstly, whether it is physically accurate to describe the tails of fatigue variability as an extrapolation of deviations from the expected mean behavior. Secondly, and a follow-up to the first question, can an increase in variability with decreasing stress level (or with respect to microstructure and other variables) be accommodated simply by broadening the lifetime probability density? Our earlier studies [7, 8, 12, 13] would suggest that a continual increase in the scale of the lifetime density is not physically plausible without being accompanied by a breakdown or some sort of separation of mechanisms.

We have discovered the so called separation of mechanisms as a function of microstructure and loading variables in several structural materials including Ti-6-2-4-6 [7, 8], γ-TiAl based alloys [12] and nickel-based superalloys [13]. This kind of response was also seen in a separate study on a β-titanium alloy [14]. These studies appear to point to an alternate theory of fatigue variability wherein the microstructure and external variables may produce different response of the mean-lifetime behavior and the life-limiting behavior in certain loading regimes. In this paper, we implement this description of fatigue variability by a bimodal probability density representing the superposition of these dual mechanisms with reference to the α+β titanium alloy, Ti-6-2-4-6. We examine the effect of microstructure and external variables on the life-limiting and the mean-dominating peaks of the bimodal density. A procedure for calculating the fatigue variability density of Ti-6-2-4-6, with respect to microstructure and loading variables, from a limited number of experiments is presented. This description is then applied in a fracture mechanics based life-prediction methodology for this material. In the end, the possible physics behind the separation of mechanisms is discussed.

2. MATERIALS AND EXPERIMENTAL PROCEDURE

2.1 Materials

The Ti-6-2-4-6 material considered in this study was in the forged pancake condition. Two different microstructures, designated as microstructures A and B, were produced. The microstructural details have been provided elsewhere [8]. Both microstructures consisted of a mixture of equiaxed (or globular) primary-α phase and lamellar α/transformed-β colonies. Besides the smaller length of lath-α and a tendency for clustering of the equiaxed-α grains in microstructure B, the two microstructures appeared similar in the electron image. The global

textures of the two (measured on a plane normal to the loading axis) were very different [8] with a greater tendency of the basal and the prismatic poles to be parallel to the loading axis in microstructure B.

2.2 Experimental Procedure

The microstructure was characterized using a LEICA field-emission scanning electron microscope (SEM). The texture was measured by Orientation Imaging Microscopy (OIM) scanning of nominal sections in the two Ti-6-2-4-6 microstructures. The scan was conducted in step-wise automated stage control to enable measurement from a relatively large area. A TSL^{TM} (a trademark of the EDAX Company) OIM camera and associated software were used for data collection and analysis. The size distribution of microstructural phases was measured using the ImagePro^{TM} image analysis program.

The Ti-6-2-4-6 specimens tested in this study were extracted in the circumferential orientation from two forging heats (with different microstructures, A and B) of the material. Cylindrical specimen geometry with a uniform gage section of about 12.5 mm length and 4 mm diameter was used for room temperature (RT) tests. For the elevated temperature (260°C) tests, cylindrical button-head specimen geometry [13] with the same gage section was used. The final machining step was low stress grinding (LSG). Each specimen was subsequently electropolished to remove approximately 50 μm from the surface in order to eliminate the LSG induced residual stress and also to produce a uniform surface.

The fatigue tests were conducted using an MTS servo-hydraulic test system with a 646 controller. The Ti-6-2-4-6 experiments were conducted at RT and 260°C. The tests were performed in load control at the frequency of 20 Hz and the stress ratio of 0.05. For the elevated temperature tests, an electric resistance furnace was mounted on the test frame. A high-

temperature button-head gripping assembly was used in conjunction with a standard collet-grip system. The hydraulic grip units were water-cooled. Temperature-control thermocouples were welded outside of the specimen gage section to maintain the test temperature at the specimen. A clip-gage was used with a few RT tests to record the stress-strain behavior. A high temperature extensometer was used with the elevated temperature tests to obtain the stress-strain loops at frequent intervals during the test.

The small crack growth experiments were also performed on round-bar specimens. The crack growth rate was monitored using the acetate replication technique. The test was interrupted at predetermined cycle intervals to obtain the replica. The specimen was held at the load of 60% of the maximum load to partially open the crack during replication. The crack lengths were measured in an Olympus^{TM} optical microscope.

The fracture surface analysis and crack initiation mechanisms were studied in a LECIA field emission SEM. The crack initiation sizes were measured using the ImagePro^{TM} program.

3. RESULTS AND DISCUSSION

3.1 A new description of fatigue variability behavior

As discussed in section 1, the traditional description of fatigue variability appears inadequate in describing the increased variability with decreasing stress level or the responses of the mean and the tails of the behavior. It was also noted, that probabilistic life prediction (for example the B0.1 lifetime) with respect to microstructure and loading variables do not appear to show physically plausible trends when based on the traditional description. Here we discuss a new, perhaps a more physics-based, description of fatigue variability behavior that may account for these trends.

The alternate description is illustrated with respect to the α+β titanium alloy, Ti-6-2-4-6. The stress vs. total lifetime behavior of microstructures A at RT is shown in Fig. 3. The deterministic range in crack growth lifetimes is also shown in the plot. The lower-bound crack-growth lifetime corresponded to upper limits of the crack initiation size and the small crack growth rate [8]. Similarly, the upper-bound lifetime was calculated from lower limits on the crack initiation size and the small crack growth rate [8]. The small crack growth behavior at 860 MPa is presented in Fig. 4. As shown, the upper and lower limits on crack growth behavior was taken as power-law segments fit to data representing the fastest and the slowest growth rate respectively. As indicated in Fig. 4, these limiting crack growth curves were taken to be the ± 3σ points in deriving the probability densities of the crack growth parameters which is discussed in section 3.2.1.

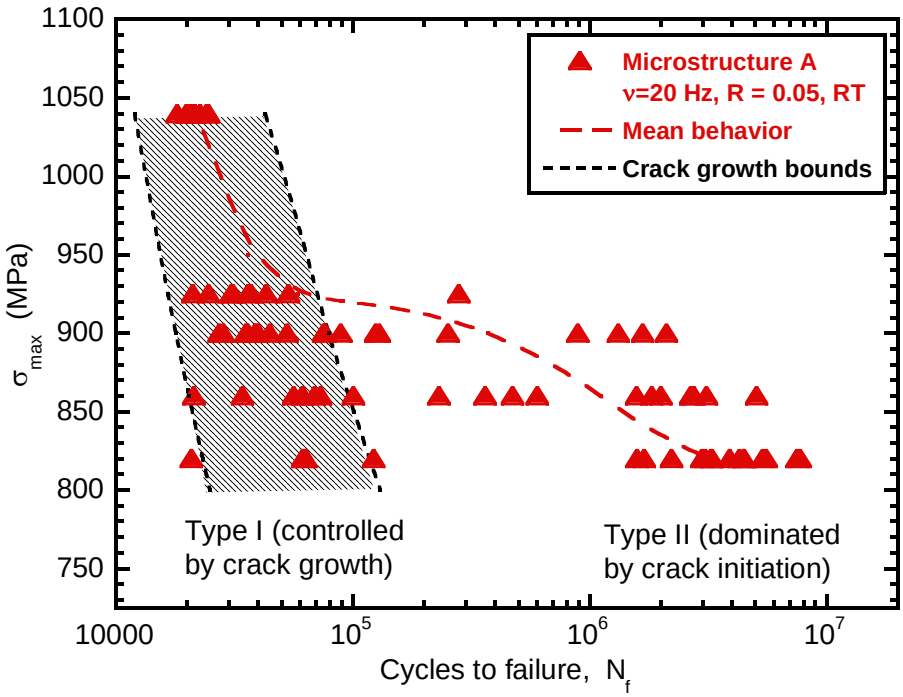

Fig. 3: Stress vs. lifetime behavior of microstructure A at RT showing the separation of crack initiation dominated behavior (Type II) from the crack growth controlled mechanism (Type I) with decreasing stress level.

Figure 3 indicates that the mean-lifetime and the life-limiting response tend to overlap with the crack growth range at the higher stress levels. With decreasing stress level, the mean behavior separated from the crack-growth-controlled (life-limiting) behavior producing increased lifetime variability at lower stress levels. In Ti-6-2-4-6 this separation can be attributed to increased dominance of crack initiation lifetime in the mean behavior [9] as the stress level is decreased.

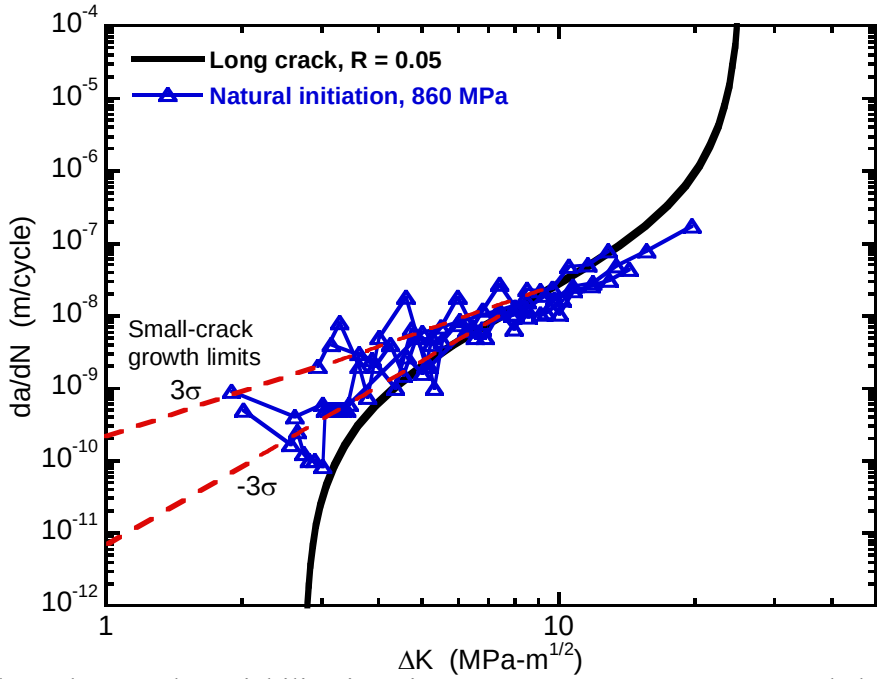

Fig. 4: Small-crack growth variability in microstructure A at 860 MPa and the crack growth limits used in the deterministic calculations.

The experimental points are plotted in the CDF space in Fig. 5 using the lognormal probability density. Only two stress levels are shown for clarity (other stress levels are given in Fig. 2(a)). The calculated crack growth ranges at both stress levels are also shown. At the higher stress level, a very good agreement of data with the CDF is seen which relates to the overlap of higher stress level behavior with the crack growth range. This agreement broke down as the stress level was decreased as illustrated by the 860 MPa points in the figure. A step-like shape of

data with respect to the CDF at the lower stress level can be shown to result from superposition of at least two mechanisms [7] at the same stress level. These mechanisms are designated as Type I and Type II in the figure. From Fig. 5, the Type I or the life-limiting behavior is controlled by crack growth. The Type II mechanism, which can be suggested to be controlled by crack initiation in Ti-6-2-4-6, dominates the mean behavior as evident from Fig. 3.

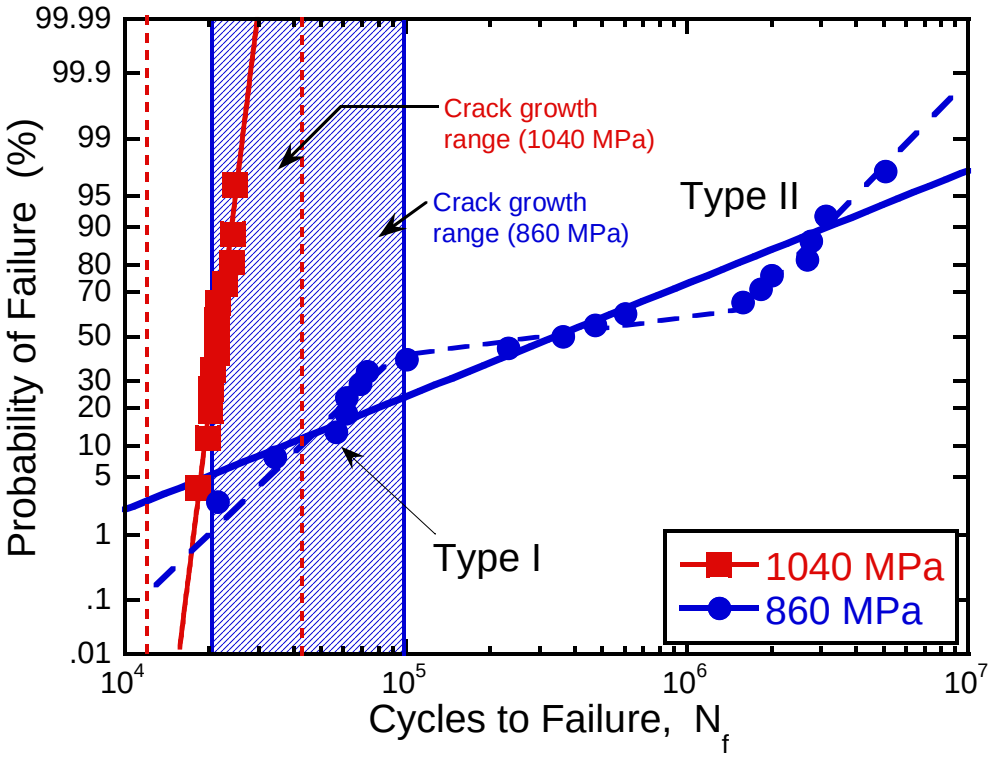

Fig. 5: Experimental points plotted in the CDF space showing the breakdown in agreement with the CDF at lower stress levels.

Based on the preceding discussion, we propose that fatigue variability behavior can be described as separation (or overlap) of a life-limiting response and a mean-lifetime dominating behavior. This is schematically illustrated in Fig. 6. Although, only the effect of stress level is illustrated in this figure, the influence of microstructure, temperature, and loading variables can also be described in terms of separate effects of these variables on the life-limiting and the mean-dominating densities, consequently affecting the total variability.

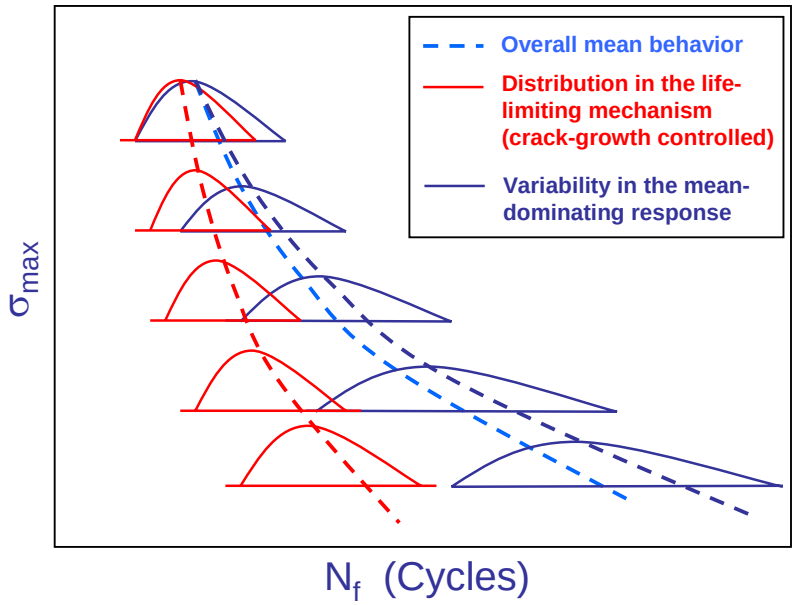

Fig. 6: Schematic illustration of the proposed description of fatigue variability behavior with respect to stress level.

3.2 Implementing the description

The proposed description of fatigue variability can be implemented by a bimodal probability density representing the superposition of a crack growth related peak and a mean lifetime dominating peak. The total density, $f_t(x)$, can be expressed as [7, 12]:

$$f_t(x) = p_l f_l(x) + p_m f_m(x) \tag{1}$$

where, $f_l(x)$ and $f_m(x)$ are the life-limiting density and the mean-lifetime dominating density respectively. These probability densities are weighted by the probability of occurrences, p_l and p_m, of individual responses such that $p_l + p_m = 1$. Here $f_l(x)$ and $f_m(x)$ are taken as the lognormal density function which is given by [15]:

$$f_{l,m}(x) = \frac{1}{xS\sqrt{2\pi}} e^{-\left(\frac{\ln x - M}{S\sqrt{2}}\right)^2} \tag{2}$$

where, M and S are the mean and the standard deviation respectively of the natural logarithm of the random variable.

3.2.1 On deriving the total probability density, $f_t(x)$

Life-limiting peak

Following the earlier discussion, the life-limiting density ($f_l(x)$) can be obtained by simulating the crack growth lifetime provided the variability in the small + long crack growth rates and the size distribution in the critical microstructural unit are known. We ran multiple small crack growth experiments using an acetate replication technique to obtain the variability in the small crack growth regime. This was illustrated in Fig. 4. In this material most of the variability in growth rates was found to occur in the early stages of crack growth, typically less than the crack length of about 30 μm [8, 16]. The variability in the small crack regime was described by the probability densities of the crack growth parameters c and m when the crack growth rate is given by [17]:

$$\frac{da}{dN} = e^{c}\Delta K^{m} \tag{3}$$

where, a is the crack size, N is cycles, and ΔK is the stress intensity factor range. The parameters c and m were assumed to be normally distributed [17] and their densities are shown in Fig. 7. In order to obtain these densities, power-law segments were fit to the small crack growth data and the ±3σ limits (where σ is one standard deviation) on the parameters c and m was taken to correspond to the small crack curves showing the maximum and the minimum average growth rates respectively (Fig. 4). The variables c and m are correlated [8] and were therefore, sampled from their joint probability density in the subsequent lifetime simulation.

Crack initiation in the life-limiting mechanism in Ti-6-2-4-6 occurred within a (or few) globular α grain(s) [18] in the specimen surface. The mean-dominating behavior comprised of a mix of surface and subsurface initiated failures [8]. These mean-behavior-contributing

mechanisms had overlapping lifetimes and acted as a group in terms of their response to operating variables [8].

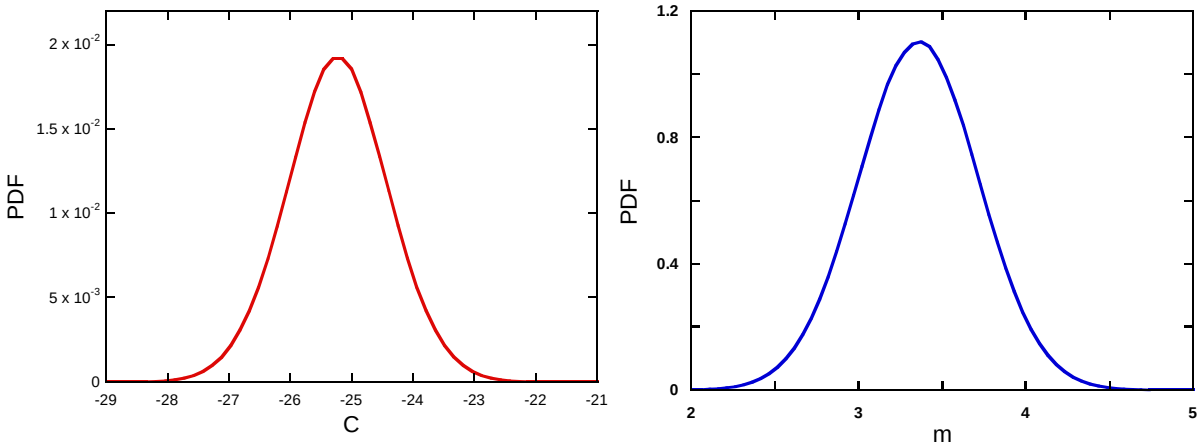

Fig. 7: Probability densities of the crack growth variables, (a) c and (b) m.

The surface replica of a small-crack growth specimen with microstructure A, recorded at N = 20,000 cycles, is shown in Fig. 8(a). The stress level was 860 MPa. The crack initiating equiaxed-α grain (about 4 μm) is indicated at the center of the crack. A (or few) crack- initiation facet(s) is typically created in the fracture surface as shown in Fig. 8(b). The sample is shown at a tilt of 45° in this figure. The distribution in the crack-initiation facet size is compared to the nominal equiaxed α size distribution in Fig. 9. The lognormal probability density function provided a good fit to the distributions as shown. Although the crack initiation sizes appear to be slightly displaced with respect to the nominal equiaxed α size distribution it is to be noted that the facet size measured in the fracture surface usually represents the largest plane across a grain [19]. The nominal distribution obtained from a metallographic section may therefore underestimate the true 3-D particle size [19]. The crack initiation size distribution along with the small-crack growth variability was employed to simulate the crack growth lifetime density ($f_l(x)$) using the Monte Carlo sampling technique.

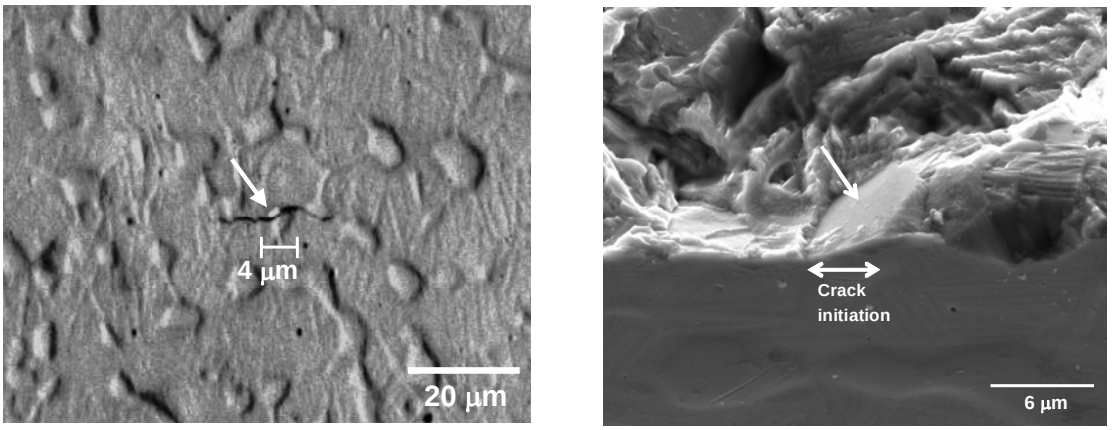

(a) (b)

Fig. 8: Crack initiation microstructural unit in Ti-6-2-4-6; (a) surface replica at N = 20,000 of a sample cycled at σ_{max} = 860 MPa with N_f =39,864 and (b) the corresponding crack initiation facet in the fracture surface.

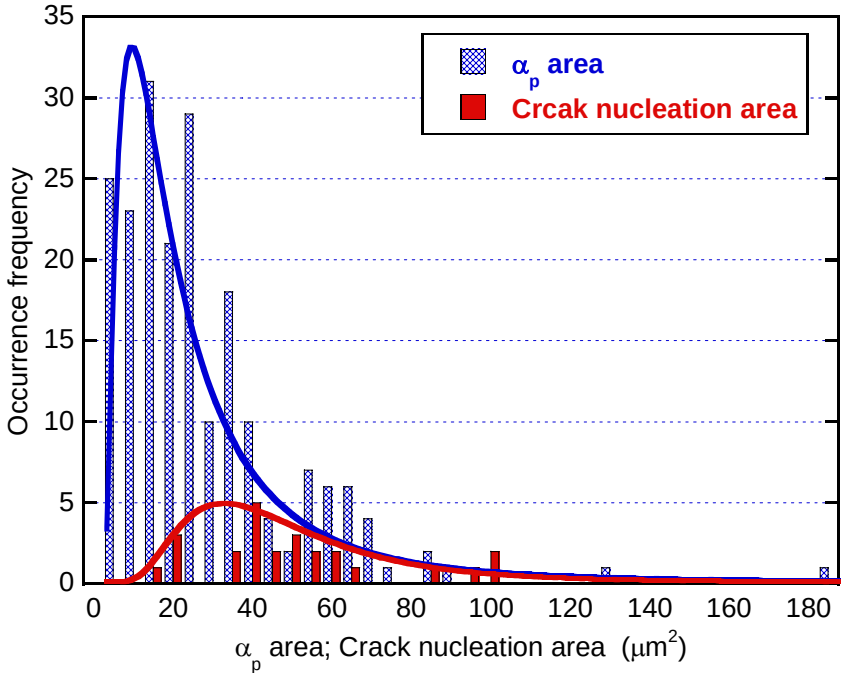

Fig. 9: Nominal equiaxed α size distribution compared to the crack initiation facet size distribution in microstructure A.

Mean-dominating peak

It may be possible to derive the mean-lifetime dominating peak, $f_m(x)$, from only a few total lifetime tests at a given stress level. This is shown for the Ti-6-2-4-6 alloy in Fig. 10. Four failure

points were randomly selected at each stress level as shown in the figure. The mean of Log(N_f) based on 10 – 19 tests at these stress levels is also plotted. The randomly selected points tend to approximately fall near the mean behavior (Fig. 10). For illustration purposes we consider the stress level of 860 MPa. In order to screen for points that may belong to the life-limiting mechanism we superimpose the simulated crack growth density at 860 MPa on the plot (Fig. 10). The points falling under the crack growth peak, within ±3σ of the mean crack growth lifetime, were classified as due to the life-limiting mechanism. The maximum likelihood estimate method [15] was then used with the remaining points to obtain the parameters of the mean-dominating (or Type II) density.

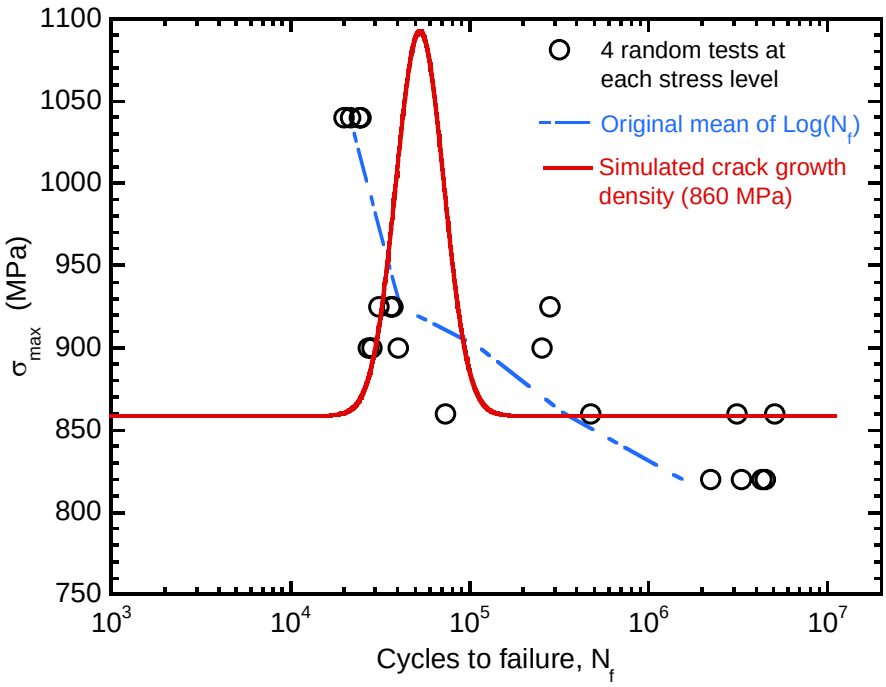

Fig. 10: Illustration of a method to derive the mean-dominating probability density, $f_m(x)$.

The crack growth (life-limiting) and the mean-dominating density at 860 MPa are shown in Fig. 11. These can be weighted by the respective probabilities, p_l and p_m, to obtain the total density, $f_t(x)$. This is shown in Fig. 12(a) for a range of values for p_l. Clearly, the heights of the

individual peaks in the total density are very sensitive to p_l and p_m (Fig. 12(a)). However, in the proposed description, the lower-tail of the density or the limiting lifetime (for example, B0.1) does not vary significantly with the probability of occurrence of mechanisms but is dependent on the parameters of the crack growth density. This is discussed further in section 3.4. The CDFs corresponding to $f_t(x)$ are shown in Fig. 12(b). Note that the ordinate is linear in this figure. Expectedly, the probability, p_l, has significant influence on the height of the step in the CDF but has a weak effect on the lower-tail behavior (Fig. 12(b)). The experimental points at 860 MPa, plotted in Fig. 12(b), are in reasonable agreement with the calculated bimodal density for p_l = 0.533 (which was the experimentally observed probability of occurrence).

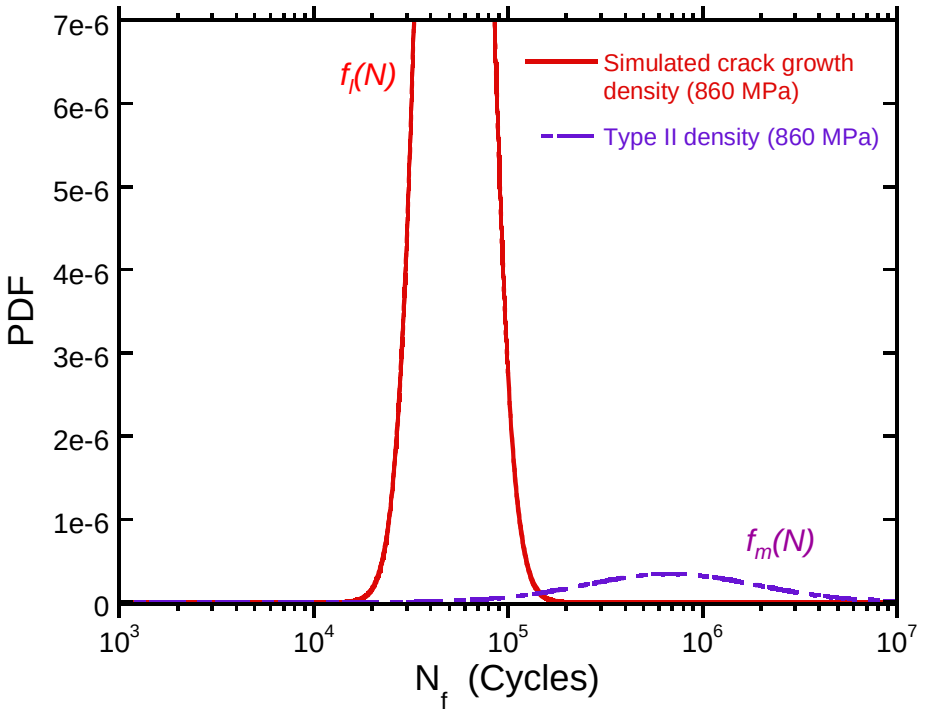

Fig. 11: Calculated life-limiting and mean-dominating densities, $f_l(x)$ and $f_m(x)$.

3.3 Understanding the effect of microstructure and loading variables on fatigue variability

The proposed description of fatigue variability behavior may be particularly useful in evaluating the effect of microstructure, temperature, and other loading variables on lifetime

variability. In case of Ti-6-2-4-6, the crack initiation and the crack growth regime will have different sensitivities to these variables. Therefore, the variables will affect the life-limiting (crack growth) and the mean-dominating (crack initiation) densities to different degrees causing their increased separation / overlap. Other variables in this study, besides the stress level, were microstructure and temperature.

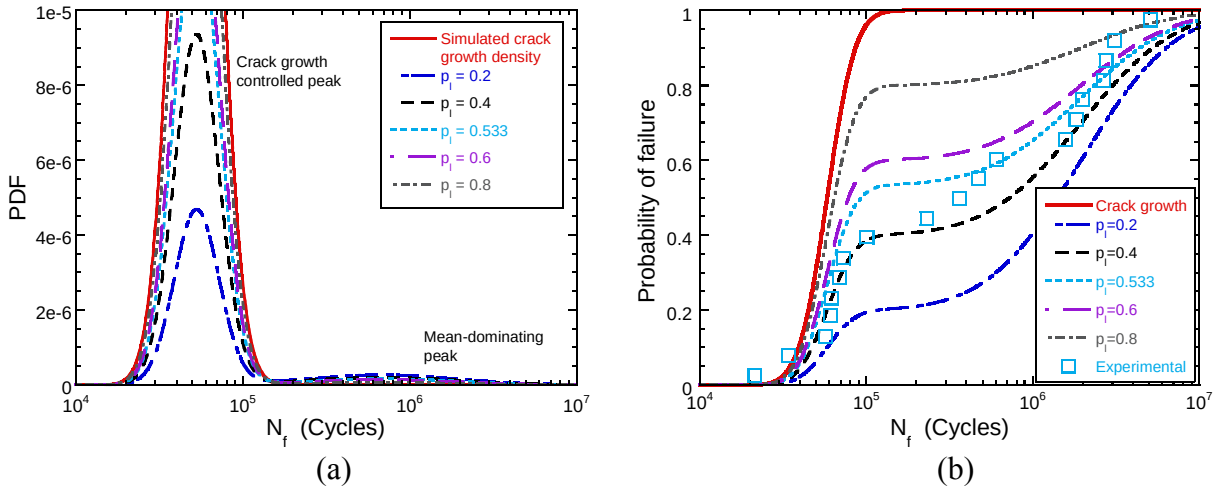

Fig. 12: The proposed description of fatigue variability behavior; (a) predicted bimodal densities with respect to p_I and (b) Effect of probability, p_I on the CDFs.

The crack growth behavior of Ti-6-2-4-6 remained almost similar in both microstructural conditions [20]. Also, an increase in the test temperature to 260°C had almost no effect on crack growth rates [20]. This is consistent with reports [21] on other α+β titanium alloys. Secondly, the surface crack initiation facets corresponded to globular α grains in both microstructures. Although we did not run small crack experiments at 260°C, the variability in small crack regime was assumed to be the same as that at room temperature. Therefore, at a given stress level, the crack growth density was similar for the two microstructures and temperatures. We randomly selected 4 samples in each microstructure and temperature condition to derive the respective mean-dominating densities using the procedure described in section 3.2.1.

The proposed description was applied to study the effect of stress level, microstructure, and temperature on lifetime variability of Ti-6-2-4-6. The effect of stress level is illustrated in Fig. 13 (a and b). The calculated probability densities are plotted for different stress levels in Fig. 13(a). The probability, p_l, used in the calculation are indicated in each case. In this figure, p_l is based on the experimental observation. Besides the probabilities, p_l and p_m, the peak heights are also very sensitive to their location and width due to the requirement of the probability density function to integrate to unity. The change in peak heights with respect to stress level can therefore, be attributed to p_l and the shift in their locations. Figure 13 (a) clearly illustrates an increase in the overlap between the mean-dominating (crack-initiation) peak and the life-limiting (crack growth) peak of the total density as the stress level is increased. At the highest stress level, 1040 MPa, it can be suggested that the two individual densities of the bimodal description are indistinguishable and the total fatigue variability can be described by the crack growth density. The corresponding calculated CDFs are compared to experiment in Fig. 13(b). The experimental points show reasonable agreement with the calculated CDFs at these stress levels although some discrepancy can be seen at higher stresses and for longer lifetimes in some cases. Note that the same small crack behavior and variability in growth rates measured at 860 MPa was used at all stress levels. A part of the discrepancy can be attributed to this assumption. Incorporation of more small-crack data in lifetime simulation is expected to further improve the agreement. Nevertheless, the predicted densities capture the effect of stress level on the tails and the total fatigue variability behavior. This indicates that the increased variability with decreasing stress level can be understood in terms of stronger response of the mean-dominating peak to stress level and therefore, increased separation from the life-limiting peak.

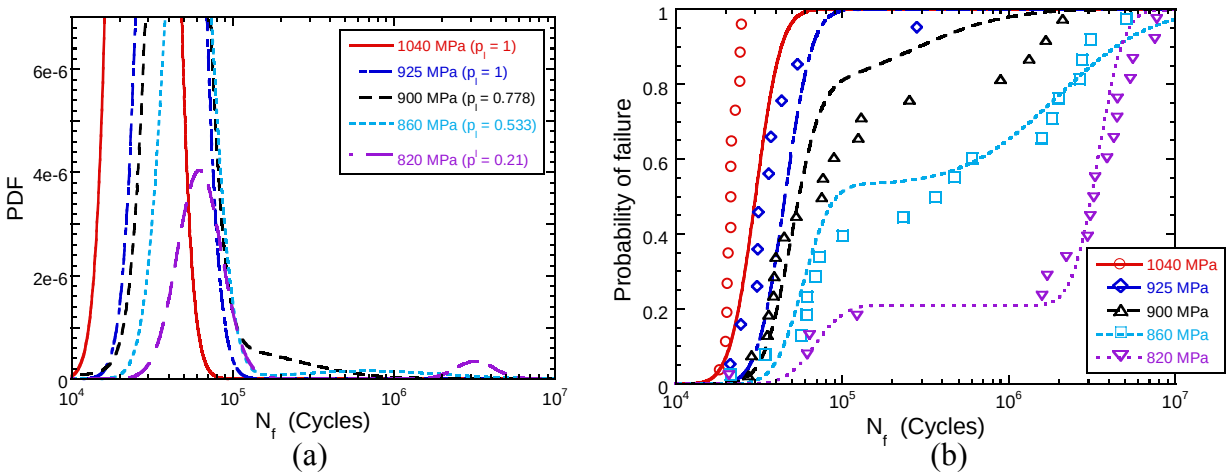

Fig. 13: Predicted fatigue variability behavior with respect to stress level; (a) calculated bimodal PDFs and (b) the corresponding CDFs compared to experiment.

Figure 14 shows that the effect of microstructure and temperature on fatigue variability can also be readily understood in terms of the sensitivity of crack growth and crack initiation regimes to these variables. The predicted total probability density at 860 MPa with respect to microstructure and temperature is presented in Fig. 14(a). The figure illustrates that the mean-dominating and the life-limiting peak shift according to the sensitivity of crack initiation and crack growth to these variables, affecting the total lifetime variability. For example an increase in temperature to 260°C has a strong influence on the crack initiation lifetime affecting the crack initiation density significantly. Since the crack growth behavior was almost unaffected by temperature, the crack growth controlled peak did not exhibit much change. The overall effect of this dual response was a decrease in the total variability with increase in temperature (Fig. 14(a)). The proposed description therefore allows for predicting the effect of these variables on lifetime distribution. The calculated CDFs with respect to microstructure and temperature are plotted in Fig. 14(b). As shown, these demonstrate reasonable agreement with the experimental points considering the assumptions made in using the small crack growth data and a relatively limited number of experimental observations.

Besides providing an understanding and prediction of the effect of microstructure and other operating variables on fatigue variability, perhaps more importantly, the proposed description may also supply a more physics-based framework for life-prediction and reliability estimates. It follows from this description that the tails of the fatigue variability behavior are not, simply a deviation from the mean behavior. In particular, the response of the lower-tail to operating variables differs from the response of the mean. From a life-prediction perspective, this would indicate that an observed decrease in total lifetime variability cannot be automatically construed as increased limiting (or B0.1) lifetime and vice versa.

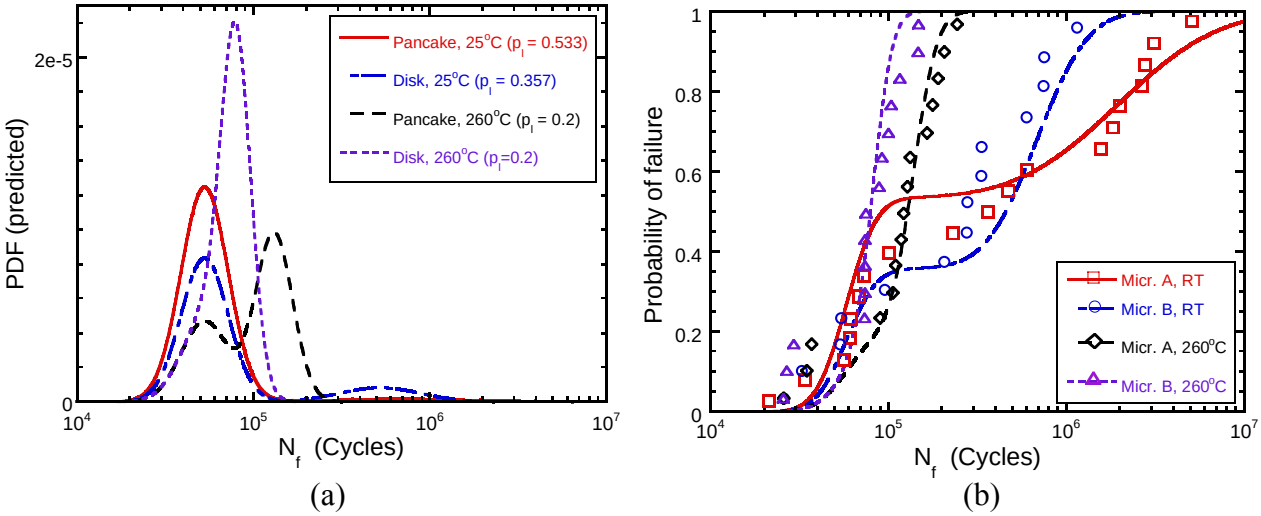

Fig. 14: Applying the bimodal density in understanding the effect of microstructure and temperature on fatigue variability; (a) calculated PDFs and (b) the corresponding CDFs compared to experiment.

3.4 Applying the description in a Life Prediction Methodology

We applied the proposed description of fatigue variability in a life-prediction approach. This approach might be more physics-based and as shown later, can produce a significant reduction in the uncertainty in life prediction. A salient factor to the application to life prediction is the understanding that fatigue variability arises from separate responses of a crack growth controlled life-limiting mechanism and a mean-dominating behavior to operating variables. Since failure

can occur by either one of the mechanisms, life-prediction can be based on the worst-case mechanism, i.e., the crack growth density in the bimodal description.

The response of the proposed lifetime density with respect to probabilities, p_l and p_m, of the superimposing behaviors was presented in Fig. 12(a). The B0.1 lifetimes derived from this bimodal probability density are plotted with respect to p_l in Fig. 15 and, as shown, appears to have a power-law relationship to p_l. The predicted B0.1 lifetime was not very sensitive to the probability of occurrence of the respective mechanisms within a range of values for p_l ($p_l \geq 0.2$) and asymptotically approached the B0.1 lifetime predicted from the crack growth density (Fig. 15). The prediction based on the crack growth density can therefore be considered as the conservative limiting lifetime. The proposed description of fatigue variability therefore, leads to life-prediction based on the crack growth density.

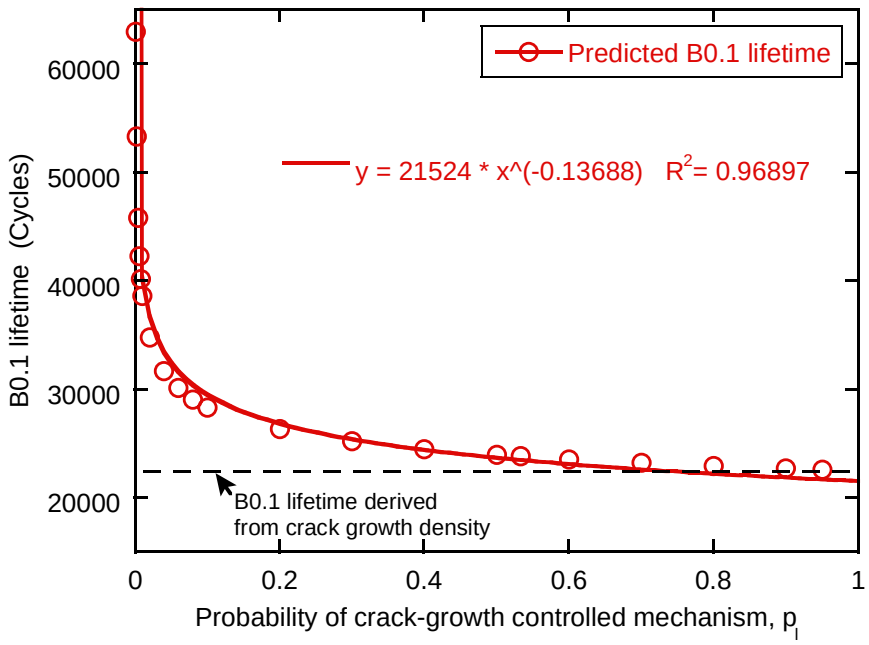

Fig. 15: The B0.1 lifetimes predicted by the proposed description of fatigue variability as a function of the probability, p_l.

The life prediction methodology is graphically illustrated in Fig. 16 for microstructure A at the stress level of 860 MPa. The predicted bimodal description is compared to the traditional description of fatigue variability in the bottom plot of Fig. 16. The traditional description was derived from the four random points at 860 MPa shown in Fig. 10 using the MLE estimates of the parameters. As discussed previously, the underlying assumption in this description is that tails of the fatigue variability behavior can be described as an extrapolation of variability with respect to the overall mean response. As such, the lower-tail behavior in this case exhibits extreme conservatism with respect to the proposed description (Fig. 16, bottom plot). The

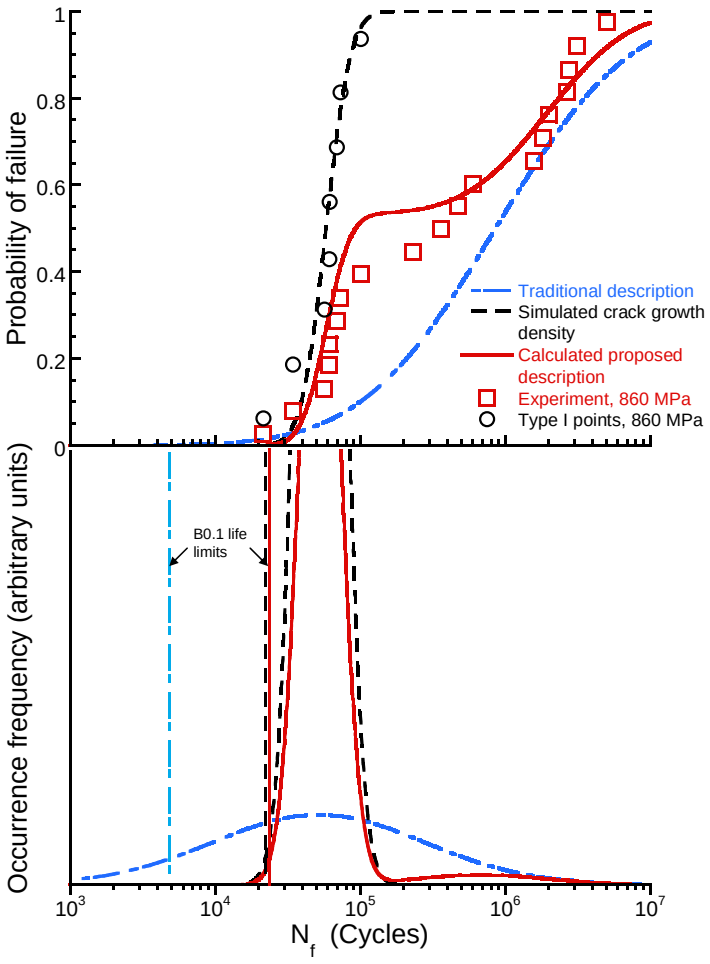

Fig. 16: Illustration of the life-prediction methodology based on the proposed fatigue variability description.

corresponding CDFs are plotted in the top plot of Fig. 16. The experimental points belonging to the Type I mechanism are plotted as separate distribution in the figure and show reasonable agreement with the calculated crack growth CDF. As expected, the B0.1 lifetime derived from the bimodal description is similar to the B0.1 life (vertical lines in the bottom plot) based solely on the crack growth density. When compared to the traditional description of fatigue variability we find a significant reduction in uncertainty with life-prediction as evident from the figure.

Although in the present instance the traditional description provided significantly conservative B0.1 lifetime, it also follows from the above discussion that a case may arise when the mean-based description produces a non-conservative prediction relative to the bimodal density. For example, this can occur when the traditional description is deduced from limited number of points that are biased towards the Type II mechanism. In either case, the proposed description of fatigue variability may produce a more accurate design lifetime.

3.4.1 Resolving the Observed Fatigue Variability Trends

The fatigue variability description developed here appears to resolve the observed trends in total variability, as a function of loading variables and microstructural constituents [10, 11], for the purpose of life-prediction. In particular, a life-prediction methodology based on the bimodal density seems to mitigate the physically counterintuitive scenarios that we alluded to previously. For example, although lower defect content increases the mean lifetime, it often produces increased lifetime variability due to non-uniform spatial distribution of initiation sites and increased scale of crack initiation size distribution [10, 11]. Similarly, in the present study we find an increase in variability with decrease in temperature from 260°C to RT (Fig. 14). If the tails of the fatigue variability behavior are considered to be an extrapolation of variability from the mean lifetime, the material with lower defect content or at the lower temperature may be

predicted to have lower limiting lifetime for given probability of failure. This is illustrated for the present Ti-6-2-4-6 alloy in Fig. 17. In the proposed description however, the lower-tail has a different behavior than the mean of the fatigue variability response, and increased variability with decreased defect content or temperature is attributed to separate response of mean-dominating mechanism from the life-limiting behavior, as shown in Fig. 17. Therefore, the limiting probabilistic lifetime at the lower temperature (or under lower defect content) is dependent on the crack growth density and is expected to be at least the same, if not higher, at RT (or in an unseeded material) than at 260°C (or a seeded condition) as shown in the figure.

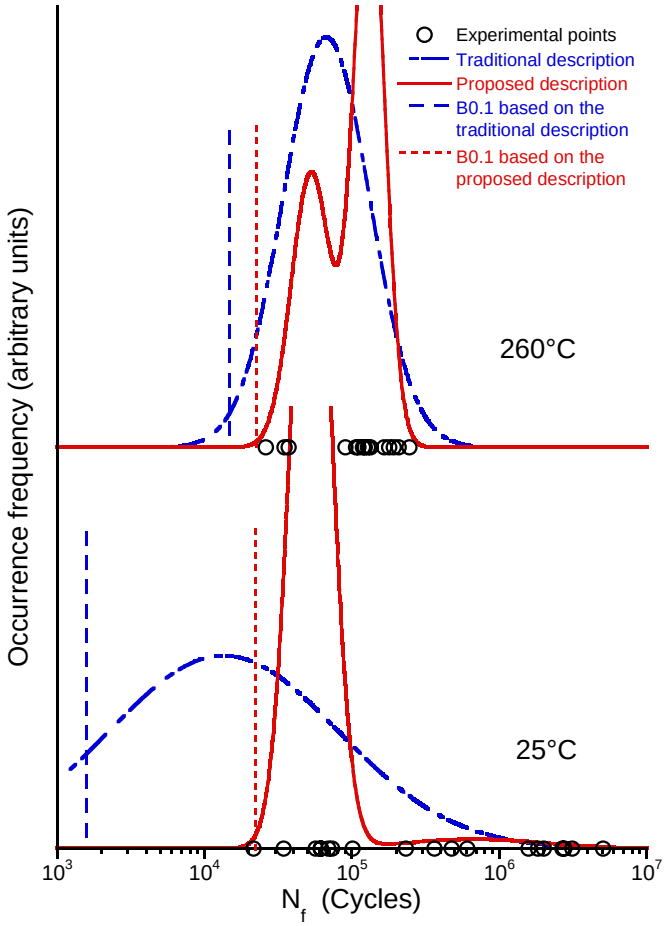

Fig. 17: Illustration of the effect of temperature on the B0.1 lifetime in the traditional and proposed description of fatigue variability.

3.5 Possible Theory of Separation of Mechanisms

We suggest that the separation of mean-dominating and life-limiting behaviors may be related to development of different heterogeneity levels in a material at the same loading condition. Analogies can be drawn from disorder – order related second order transitions that is seen in several physical systems including ferromagnetism [22] and earthquake dynamics [23, 24], and it may be possible to apply the statistical physics based theories from these fields to fatigue variability behavior.

At the highest stress level (1040 MPa), Ti-6-2-4-6 may be considered to produce a relatively homogeneous deformation response to applied stress. As such, the life-limiting and the mean-dominating behaviors seem to completely overlap and single mode is observed. At the lower stress level, heterogeneity levels are generated in the material due to local plasticity. The localized deformation can be attributed to several factors, from favorable crystallographic orientation of a grain [25] or collection of grains [26] to clustering of microstructural phases [14] and grain boundary disorientation [27]. These factors are, of course, material and loading dependent. If the underlying physics of fatigue variability is similar to the statistical-physics systems mentioned above, several of these factors can be suggested to be operational at a given applied stress causing a ranking of heterogeneity levels. It is also known that some of the initial stress concentration may decay with cycles due to, for example, slip transfer to less favorably oriented regions [29] causing relatively more uniform distribution in deformation with time. It can be speculated that, this evolution of heterogeneity levels presents a finite probability of crack initiation in randomly-occurring critical microstructural neighborhoods within the initial cycles causing a crack growth controlled mechanism. The mean-dominating behavior, on the other hand, is suggested to be realized by damage accumulation at a much smaller and therefore, more

frequently distributed heterogeneity scale than the life-limiting mechanism. As shown previously, this is dominated by crack initiation lifetime in Ti-6-2-4-6. These mechanisms can be suggested to operate in sequence and the mean-behavior is realized only after the life-limiting mechanism is not encountered. Clearly, the probability of occurrence of the crack growth controlled mechanism will vary depending on the material and external variables but, we suggest it is important to probabilistically account for this theoretical possibility and incorporate it in life-prediction.

4. CONCLUSIONS

The following main conclusions can be drawn from this study:

(i) The fatigue variability is realized by separate response of crack-growth-controlled, life-limiting mechanism, and mean-dominating behavior (controlled by crack initiation in Ti-6-2-4-6) to microstructure and loading variables.

(ii) This description can be implemented by a bimodal probability density representing superposition of crack growth and mean-dominating densities. The bimodal density can be calculated from simulated crack growth density and few total lifetime tests.

(iii) The proposed description can prove very useful in understanding the effect of microstructure, temperature, and other variables on fatigue variability.

(iv) In the limiting case, the B0.1 lifetime obtained from the bimodal density approaches the B0.1 lifetime derived solely from the crack growth density providing a fracture mechanics basis for life-prediction methodology.

(v) The seemingly counterintuitive effects of defect content, temperature, and loading variables on probabilistic life-prediction could be resolved in the proposed description of fatigue variability.

ACKNOWLEDGEMENTS

This work was performed at the Air Force Research Laboratory, Materials and Manufacturing Directorate, Wright-Patterson Air Force Base, OH. The partial financial support of the Defense Advanced Research Project Agency (DARPA) under DARPA orders M978, Q588, P699, and S271 with Dr. Leo Christodoulou as the program manager is gratefully acknowledged. We acknowledge Mr. Phil Buskohl and Ms. Lindsey Selegue for their assistance with the replication-based small-crack growth experiments. We also wish to acknowledge Dr. Mike Caton and Dr. Reji John for very helpful discussions.

REFERENCES

[1] K. S. Chan and M. P. Enright, *Journal of Engineering for Gas Turbines and Power*, Vol. 124, pp. 889-885, 2006.

[2] R. Tryon and A. Dey, *J. Aerospace Engng.*, p.120, 2001.

[3] H. Yokoyama, O. Umezawa, K. Nagai, and T. Suzuki, *ISIJ International*, Vol. 37, p. 1237, 1997.

[4] J. W. Lincoln, *Journal of Aircraft*, Vol. 22, 1985.

[5] J. N. Yang and W. J. Trapp, *AIAA Journal*, Vol. 12, pp. 1623-1630, 1974.

[6] L. Christodoulou and J. M. Larsen, *JOM*, Mar 2004, p. 15, 2004.

[7] S. K. Jha, J. M. Larsen, A. H. Rosenberger, and G. A. Hartman, *Scripta Materialia*, Vol. 48, p. 1637, 2003.

[8] S. K. Jha, M. J. Caton, and J. M. Larsen, *Materials Science and Engineering A*, article in press, DOI: 10.1016/j.msea.2006.10.171, 2007.

[9] J. Ruppen, D. Eylon, and A. J. McEvily, *Metall. Trans. A*, Vol. 11A, p. 1072, 1980.

[10] T. P. Gabb, J. Telesman, P. T. Kantzos, P. J. Bonacuse, and R. L. Barrie, *NASA/TM-2002 211571*, 2002.

[11] J. Huang, J. E. Spowart, and J. W. Jones, *Fatigue Fract. Engng. Mater. Struct.*, Vol. 29, pp. 507-517, 2006.

[12] S. K. Jha, J. M. Larsen, and A. H. Rosenberger, *Acta Materialia*, Vol. 53, p. 1293, 2005.

[13] M. J. Caton, S. K. Jha, J. M. Larsen, and A. H. Rosenberger, in *Superalloys 2004*, 2004.

[14] K. S. Ravi Chandran and S. K. Jha, *Acta Materialia*, Vol. 53, p. 1867, 2005.

[15] W. Q. Meeker and L. A. Escobar, in *Statistical Methods for Reliability Data*, Wiley Series in Probability and Statistics, 1998.

[16] S. K. Jha, J. M. Larsen, and A. H. Rosenberger In: *Fatigue 2006*, International Fatigue Congress, Atlanta, GA, 2006.

[17] C. G. Annis, In: *Probabilistic aspects of life prediction*, ASTM STP 1450, W. S. Johnson, and B. M. Hillberry, Eds., ASTM International, West Conshohocken, PA, 2004.

[18] S. K. Jha, J. M. Larsen, A. H. Rosenberger, and G. A. Hartman, ASTM, STP 1450, W. S. Johnson, and B. M. Hillberry, Eds., ASTM International, West Conshohocken, PA, 2004.

[19] R. L. Fullman, *Trans. AIME*, Vol. 197, p. 447, 1953.

[20] S. K. Jha, J. M. Larsen, and A. H. Rosenberger, unpublished research, Air Force Research Laboratory, Dayton, OH.

[21] NASA Technical Report, NASA/TM 2001-210830.

[22] K. H. Hoffman and M. Schreiber, Eds., Computational Statistical Physics, Springer Publ., pp.211-226, 2002.

[23] J. B. Rundle, D. L. Turcotte, R. Shcherbakov, W. Klein, and C. Sammis, *Review of Geophysics*, Vol. 41, pp. 1019, 2003.

[24] D. Sornette, Proceedings of the National Academy of Sciences of the United States of America (PNAS), Vol. 99, Suppl. 1, 2522-2529, 2002.

[25] P. Lukas, M. Klesnil, and J. Polak, Mater. Sci. Engng, Vol. 15, pp. 229-245, 1974.

[26] C. J. Szczepanski, S. K. Jha, J. M. Larsen, and J. W. Jones, In Press, VHCF-4, Proceedings of the 4th international conference on very high cycle fatigue, Ann Arbor, MI, 2007.

[27] D. L. Davidson, R. Tryon, M. Oja, K. S. Ravi Chandran, TMS Annual Meeting, San Antonio, TX, 2006.

[28] X. Feaugas and M. Clavel, *Acta Materialia*, Vol. 45, pp. 2685, 1997.